Insight into prediction of unsteady forced convection in a porous straight channel subject to inlet flow modulation: A REV lattice Boltzmann investigation.

Hassane NAJI [1*], Riheb MABROUK [2], Hacen DHAHRI [2]

[1]Univ. Artois, IMT Nord Europe, Junia, Univ. Lille, ULR 4515, Laboratoire de Génie Civil et géo-Environnement (LGCgE)
F - 62400 Béthune (France)
[2]Université de Monastir, École Nationale d'Ingénieurs de Monastir, Laboratoire d'Études des Systèmes Thermiques et Énergétiques (LESTE)
Rue Ibn Jazza - 5019 Monastir (Tunisia)
[*](Corresponding author: hassane.naji@univ-artois.fr)

Abstract - A thermal mesoscopic method at a representative elementary volume scale level is taken up to numerically address the problem of an unsteady forced convection in a porous straight channel subjected to an inlet flow modulation. The thermal lattice Boltzmann method (TLBM) enthalpy-based is employed to deal the Brinkman- Forchheimer - Darcy (BFD) and two-energy models. Relevant values of the pulse amplitude A, porosity ε and Strouhal number St were deemed. Velocity-contours, solid-fluid difference temperature, streamlines, and melt front progress are exhibited.Based on the findings, it can be stated the melting slows down for larger A and St number at the porosity deemed.

Nomenclature

A	pulsating amplitude
Bi	Biot number
Br	Brinkman number, $\mathrm{Br} = \mathrm{Pr}.\mathrm{Ec}$
c	lattice speed, $\mathrm{m.s^{-1}}$
C_p	specific heat capacity, $\mathrm{kJ.kg^{-1}.K^{-1}}$
c_s	sound speed, $\mathrm{m.s^{-1}}$
Ec	Eckert number
Da	Darcy number
e_i	discrete velocity in direction i
F_{ei}	discrete body force, $\mathrm{kg.m^{-3}.s^{-1}}$
f_i, g_i	distribution functions
K	porous medium permeability, m²
Kr	thermal conductivity ratio
La	latent heat, $\mathrm{J.kg^{-1}}$
P	dimensionless pressure
Pr	Prandtl number
Rc	heat capacity ratio
Re	Reynolds number
Ste	Stefan number
St	Strouhal number
T	température, K
T_m	PCM melting temperature, K
$\tilde{t}$	dimensionless time
$\vec{U}$	dimensionless velocity along X-direction
U_0	initial velocity
w	pulsation, $\mathrm{rd.s^{-1}}$
X, Y	dimensionless coordinates

Greek symbols

α	thermal diffusivity, $\mathrm{m^2.s^{-1}}$
∇	gradient operator
$\nabla.$	divergence operator
δt	time step
Γ	PCM's melting fraction
ε	porous medium's porosity
λ	thermal conductivity, $\mathrm{W.m^{-1}.K^{-1}}$
ν	kinematic viscosity, $\mathrm{m^2.s^{-1}}$
ρ	density, $\mathrm{kg.m^{-3}}$
τ	Dimensionless relaxation time
Θ	dimensionless temperature

Superscripts/subscripts

c	cold
eff	effective
f	fluid
h	hot
o	reference
s	solid

https://doi.org/10.25855/SFT2022-082

1. Introduction

Pulsating flow, as a common phenomenon in both natural and engineering systems, has received extensive attention. In addition, the technologies involving unsteady forced convection with phase change in porous media with unsteady inlet flow are increasingly investigated. Fluid flows and heat transfer in porous composite media comprising phase change materials (PCM) have aroused growing interest in recent decades mainly due to its fundamental significance and their many applications, such as thermal energy storage, electronics cooling, melting/solidifying in porous media, solar energy use, building heating, nuclear reactors, and so on.

Now, it is well known that thermal energy storage systems (TESSs) have tremendous potential for an economic use of thermal equipment and large-scale energy substitution. Of all the TESS available, the most attractive is the latent heat thermal energy systems (LHTESs). From a technical point of view, heat transfer under pulsed flow is often found in various industrial applications [1, 2] such as finned heat sinks for electronic chipsets, filtration devices, pulsed tube cryo-coolers, ducted air conditioners, aerosols transport in human respiratory tract, blood flow in the vessels, etc. Sometimes, the system is modulated by sin waves superimposed on a time-varying input flow. The thermal energy storage mitigates the time gap between supply and demand, improves the energy systems performance and helps conserve energy. This storage can be achieved by using several heat kinds (sensible, latent, etc.). Of these, latent thermal energy storage (LHES) via PCMs remains the most preferred and used method because these materials can store or release energy over a tiny temperature range. Paraffin is a PCM that still arouses interest in terms of research and use. However, due to its low thermal conductivity, metal foams have been added to fill this weak point. Thereby, they have become a complementary support for further improving heat transfer due to their high thermal conductivity [3, 4].

Deng *et al.* [5] numerically and experimentally studied the melting PCM' melting in a porous metallic foam and examined the effects of many parameters including porosity and fractal dimension on the melting heat transfer. They demonstrated that interstitial heat transfers at the PCM/matrix interface for melting behaviors is essential. Ghalambaz and Zhang [6] studied the effect of pulsed thermal load on the cooling performance and energy storage/release of a heat sink filled with metallic foam. Jafari *et al.* [7] used a lattice Boltzmann method (LBM) based on dual population approach and bounce back method to numerically investigate effects of single-walled carbon nanotubes (SWCNT) on convection heat transfer in a corrugated channel with a pulsating inlet velocity. They found that the pulsed flow improves the heat transfer and that the pulsation rate performance is highly dependent on the Reynolds number, amplitude and frequency.

In addition to experimental studies, numerical studies have been and continue to be performed to handle unsteady fluid flows and heat transfers in porous media. However, modelling and numerical simulation of these problems remains a challenging task due to the non-linear characteristics of phase change process and the porous structure complexity. In this context, to perform numerical simulations, the LBM, which has greatly developed over the two decades, appeared as a power approach for studding complex flows, heat transfer and other complicated physics. Compared to the traditional methods of computational fluid dynamics, the LB method has some indisputable advantages, including advanced algorithms incorporation, programming simplicity, computational locality and ease of handling complex boundaries conditions such as those of porous media. In this method, the fluid consists of a particles' number that stream and interact in certain specified directions depending on the lattice structure. Note that, the LBM at the representative element volume (REV) is accomplished by including an additional term to translate the composite medium (porous medium with a PCM) presence. The pore-scale simulation being not straightforward to apply for LHTESs even miniaturized, flow simulation based on the REV approach has a significant advantage in large-scale simulation. To date, the concept of REV has been widely accepted and successfully applied in many fields.

To the best of our knowledge, studies of pulsed flows with phase change within a porous system (e.g. channels) with thermal lattice Boltzmann method at the REV scale remain scarce.

The novelty of this work is twofold: a) to fill this scarcity, and b) to extend the TLBM to cope with the unsteady forced convection in a porous medium containing a PCM embedded in an open channel under the condition of local thermal non-equilibrium (LTNE). For this, three distribution functions were deemed to simulate the velocity field and temperature fields of the fluid and of the solid matrix.

The physical model considered here consists of a rectangular metal-foam (porous) channel including a PCM whose height is H and the length is L. The flow is assumed to be unsteady, incompressible, 2D, and subjected to a sin and time-varying input flow. In addition, the thermo-physical properties of the fluid and the porous matrix are assumed to be constant, and the fluid-saturated porous medium is considered homogeneous, isotropic, non-deformable, and in LTNE with the fluid. With this, the heat transfer due to radiation and natural convection is presumed to be negligible.Thereby, to model such a problem, we consider the generalized dimensionless Navier-Stokes equations for a porous media [8, 9]. To fill up the problem formulation, the enthalpy-porosity model was adopted to calculate the PCM liquid fraction. Note that the problem has a melting temperature (inlet temperature), and initially, both metal foam and paraffin are at equilibrium and the entire channel is at the low temperature (outlet temperature).

The remainder of this paper is organized as follows. Section 2 presents the governing equations' set along with appropriate boundaries conditions (BCs) to be solved. The put up thermal SRT-LBM with three distribution functions is outlined in Section 3. Thereafter, Section 4 presents and comments our predictions. Finally, major conclusions are drawn in Section 5 from numerical simulations.

2. Mathematical formulation and problem statement

To simplify the problem, the investigated physical set-up is a PCM-filled planar porous channel of length L and height H (Figure 1). The fluid (air) enters the channel at high temperature T_h with a pulsating velocity while initiating the paraffin melting start, and exits cold at the temperature $T_c\,(<T_h)$. The top and bottom walls are thermally insulated. The outlet conditions are assumed to be fully developed. It is noteworthythat the melting point of the PCM is T_m and that at the initial time, the left wall temperature is raised to T_h $(T_h > T_m)$ thereby starting the melting of the PCM.

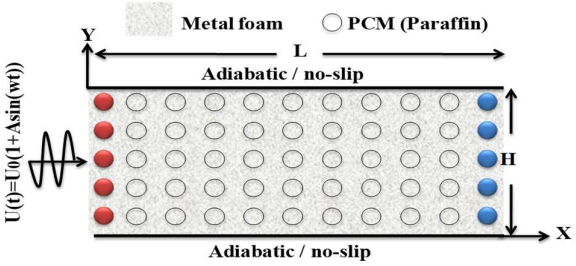

Figure 1: *Computational domain of a LHTES channel along with boundary conditions.*

Based on the up-mentioned assumptions, the Brinkman-Forchheimer-Darcy (BFD) and LTNE energy equations in porous media can be presented in the following tensorial form [8 -10]:

$$\nabla\cdot\vec{U}=0 \tag{1}$$

$$\partial\vec{U}/\partial\tilde{t}+\left(\vec{U}.\nabla\right)\left(\varepsilon^{-1}\vec{U}\right)=-\nabla\left(\varepsilon P\right)+Re^{-1}\nabla^2\vec{U}-\varepsilon.\left(Re^{-1}.Da^{-1}+F_\varepsilon Da^{-1/2}\left\|\vec{U}\right\|\right)\vec{U} \tag{2}$$

$$\partial\Theta_f/\partial\tilde{t}+\vec{U}.\nabla\Theta_f=\frac{1}{Re.Pr}\nabla.\left(\frac{\lambda_{eff,f}}{\lambda_f}\nabla\left(\frac{\Theta_f}{\varepsilon}\right)\right)+Kr.\frac{Bi}{Re.Pr}\left(\frac{\Theta_s-\Theta_f}{\varepsilon}\right)-Ste^{-1}\partial\Gamma/\partial\tilde{t}+\tilde{\Phi} \tag{3}$$

$$\partial\Theta_s/\partial\tilde{t}=\frac{Kr}{Rc}\frac{1}{Re.Pr}\nabla.\left(\frac{\lambda_{eff,s}}{\lambda_s}\nabla\left(\frac{\Theta_s}{1-\varepsilon}\right)\right)-\frac{Kr}{Rc}.\frac{Bi}{Re.Pr}\left(\frac{\Theta_s-\Theta_f}{1-\varepsilon}\right) \tag{4}$$

where $\vec{U}(U,V)$ and P are the volume-averaged velocity and pressure over the computational cell. ε and $\vec{F}$ denote the porous medium's porosity and the total force due to its presence and other external forces. Θ_f and Θ_s are the fluid and porous medium temperatures, Γ and $\tilde{\Phi}$ are the PCM liquid fraction and the viscous dissipation, respectively, and λ_{eff} is the effective thermal conductivity.

F_ε and K can be written as $F_\varepsilon = 2.12\times10^{-3}(1-\varepsilon)^{-0.132}(d_f/d_p)^{-1.63}$ where $d_f = 1.18\left((1-\varepsilon)/3\pi\right)^{1/2} d_p$ and $d_p = 22.4\times10^{-3}/\varpi$ and $K = 7.3\times10^{-4} d_p^2(1-\varepsilon)^{-0.224}(d_f/d_p)^{-1.11}$, K being the porous medium permeability. Here, d_f, d_p and ϖ are the ligament diameter, the pore size, and the pore density, respectively.

The PCM viscous dissipation (Eq. (3)) can be expressed as follows:

$$\tilde{\Phi} = \varepsilon.Ec\left\{\frac{1}{Da.Re} + \frac{F_\varepsilon}{\sqrt{Da}}\left\|\vec{U}\right\|\right\}\left\|\vec{U}\right\|^2 + \frac{Ec}{Re}\left\{2\left[\left(\frac{\partial\vec{U}}{\partial X}\right)^2 + \left(\frac{\partial\vec{V}}{\partial Y}\right)^2\right] + \left(\frac{\partial\vec{U}}{\partial Y} + \frac{\partial\vec{V}}{\partial X}\right)^2\right\} \tag{5}$$

The associated dimensionless boundary and initial conditions (BCs & ICs) are as follows:

$$At\ \tilde{t} > 0: U(\tilde{t}) = 1 + A\sin(2\pi St.\tilde{t});\ V = 0;\ \Theta_{f,h} = 1,\ at\ X = 0\ \ and\ 0 \le Y \le 1\ (inlet) \tag{6}$$

$$\Delta_X U = 0;\ V = 0;\ \Theta_{f,c} = 0,\ at\ X = L/H\ \ and\ 0 \le Y \le 1\ (outlet) \tag{7}$$

$$U = 0;\ V = 0\ and\ \nabla_y\Theta_{f,h} = \nabla_y\Theta_{f,s} = 0\ at\ 0 \le X \le L/H,\ Y = 1\ (top)\ and\ Y = 0\ (bottom) \tag{8}$$

$$At\ \tilde{t} = 0,\ U = 0;\ V = 0;\ \Theta_f = 0\ (IC) \tag{9}$$

To deal with the physical problem, the following dimensionless variables have been used:

$$(X,Y) = (x,y)/H,\ (U,V) = (u,v)/U_0,\ P = p/\rho U_0^2,\ \tilde{t} = tU_0/H,\ \Theta = (T-T_c)/(T_h-T_c) \tag{10}$$

So, the up Eqs. (1) - (4) are characterized by the following key dimensionless parameters:

$$\begin{aligned} &Bi = h_{sf}a_{sf}H^2/\lambda_s,\ Da = K/H^2,\ Ec = U_0^2/C_f\Delta T_{ref},\ Kr = \lambda_s/\lambda_f,\ Pr = \nu_f/\alpha_f,\\ &Rc = (\rho C_p)_s/(\rho C_p)_f,\ Re = U_0H/\nu_f,\ Ste = C_{p,f}(T_h - T_m)/La,\ St = \breve{f}H/U_0 \end{aligned} \tag{11}$$

It is worth mentioning that the interstitial heat transfer (h_{sf}) and the porous matrix specific surface area (a_{sf}) are computed via the commonly used empirical relationships [11]:

$$h_{sf} = \begin{cases} 0.76.Re_d^{0.4}\,Pr^{0.37}\,\lambda_f/d_f \\ 0.52.Re_d^{0.5}\,Pr^{0.37}\,\lambda_f/d_f \\ 0.26.Re_d^{0.6}\,Pr^{0.37}\,\lambda_f/d_f \end{cases} \quad for \quad \begin{cases} 1 \le Re_d \le 40 \\ 40 \le Re_d \le 10^3 \\ 10^3 \le Re_d \le 2.10^5 \end{cases} \tag{12}$$

$$a_{sf} = 3\pi d_f(1 - e^{-(1-\varepsilon)/0.004})/0.59/d_p^2 \tag{13}$$

Note that the meaning for the symbols are outlined and listed in nomenclature.

The liquid fraction Γ is computed using the following relationship from the enthalpy method [12, 13], to name a few: $\Gamma = \begin{cases} 0 & \Theta < \Theta_s \\ (\Theta - \Theta_s)/(\Theta_l - \Theta_s) & if\ \ \Theta_s \le \Theta \le \Theta_l \\ 1 & \Theta > \Theta_l \end{cases}$ (14)

3. Thermal lattice Boltzmann method

The Lattice-Boltzmann (LB) method has become increasingly popular for simulating fluid dynamics and heat transfer. Unlike the Navier-Stokes methods which directly describe the dynamics of macroscopic flow quantities (e.g. momentum, pressure, etc.), it is a statistical

approach originally derived from lattice-gas models. It consists of the spatio-temporal discretization of the Boltzmann equation from which the Navier-Stokes equations can be recovered through the multi-scale Chapman-Enskog expansion analysis [14], details of which can be found in the Refs. [15, 16], to name a few.

In the REV-LBM for thermal flows, the multi-distribution functions (MDF) approach is extensively used due to its good numerical stability and simplicity. In this framework, the velocity field and thermal fields within the PCM and solid matrix are handled separately using a specific distribution function (for each field).

3.1. LB equation for fluid flow in porous medium

In the Bhatnagar-Gross-Krook (BGK) approximation, the common form of the LB equation for a distribution function can be written as [17]:

$$f_i\left(x+e_i\delta t,t+e_i\delta t\right)-f_i\left(x,t\right)=-\delta t\omega_i\left(f_i-f_i^{eq}\right)\left(x,t\right)+\delta tF_{e_i} \tag{15}$$

where $\omega_i\,(=1/\tau_v)$ is the single relaxation collision frequency, $\tau_v\,(=3\nu+0.5)$ being the dimensionless relaxation time; e_i is the discrete velocity in direction i, $f_i(x,t)$ is the density distribution function with velocity e_i at position x and time t, δt is the time increment, and $f_i^{eq}(x,t)$ is the equilibrium distribution function (EDF), which, for the well-known D2Q9 lattice model, can be defined as follows:

$$f_i^{eq}=\rho w_i\left(1+e_iu/c_s^2+uu:\left(e_ie_i-c_s^2I\right)/2c_s^4\varepsilon\right) \tag{16}$$

where w_i is the weight, $c_s\,(=c/\sqrt{3})$ is the sound speed and I is the unit tensor. For the D2Q9 model adopted here, w_i are set as: $w_0=4/9$, $w_{1,4}=1/9$ and $w_{5,8}=1/36$.

3.2. TLB equation for temperature fields of the PCM and solid matrix

The SRT-LBM equations for temperature fields of the PCM and solid matrix can be written as [18]:

$$\begin{aligned}g_{f,i}\left(x+e_i\delta t,t+\delta t\right)-g_{fi}\left(x,t\right)=&-\omega_{T,f}\left(g_{fi}\left(x,t\right)-g_{fi}^{eq}\left(x,t\right)\right)\\&+\left(1+\delta t\partial_t/2\right)\delta tw_i\left(\frac{La}{C_{p,f}}\left(\frac{\gamma(t+\delta t)-\gamma(t)}{\delta t}\right)+\frac{h(T_s-T_f)}{\varepsilon(\rho C_p)_f}\right)\\&+\delta tf_i\left(x,t\right)\left[\left(f_i-f_i^{eq}\right)\left(e_i-u\right)\left(e_i-u\right):\nabla u\right]\end{aligned} \tag{17}$$

$$g_{si}\left(x+e_i\delta t,t+\delta t\right)-g_{si}\left(x,t\right)=-\omega_{T,s}\left(g_{si}\left(x,t\right)-g_{si}^{eq}\left(x,t\right)\right)+\left(1+\delta t\partial_t/2\right)\delta tw_i\left(\frac{h(T_s-T_f)}{(1-\varepsilon)(\rho C_p)_s}\right) \tag{18}$$

where the subscripts f and s denote the fluid and solid phases, respectively. Here, $g_{f,i}$ and $g_{f,i}^{eq}$ are the temperature distribution function and the equilibrium temperature distribution function, respectively. $\omega_{T,f;s}\,(=1/\tau_{T,f;s})$ is the single relaxation collision frequency for temperature distribution function, $\tau_{T,f;s}$ being the dimensionless relaxation times set as:

$$\tau_{T,f}=3\alpha_{e,f}/(\delta tc^2)+0.5\quad and\quad \tau_{T,s}=3\alpha_{e,s}/(\delta tc^2)+0.5 \tag{19}$$

with $\alpha_{e,f}=k_{e,f}/\left(\varepsilon(\rho C_p)_f\right)$ and $\alpha_{e,s}=k_{e,s}/\left((1-\varepsilon)(\rho C_p)_s\right)$ pointing out PCM (in the fluid state) and solid matrix effective diffusivities, respectively.

Based on the distribution functions, the local density ρ, velocity and temperatures are obtained via the following relationships:

$$\rho=\sum_i f_i,\ u=\sum_i f_ie_i/\rho+\delta tF_{e_i}/2,\ T_f=\sum g_{f,i}\ and\ T_s=\sum g_{s,i} \tag{20}$$

Note that the BCs and ICs specified above (see Section 2) have been converted (at the mesoscopic level) to the usual bounce-back condition.

The LBM simulation(flow chart)is mainly split into three steps for each lattice node at each time-instant. The first is a simple propagation of distribution functions in discrete directions (cf. the left hand side of Eqs. (15), (17) and (18)). In the second, the BCs and the collision (relaxation) terms for the density and energy distribution functions are applied, while in the last step, the computation of macroscopic quantities from Eqs. (20), and finally, findings gathering are performed.

4. Results and discussion

Before presenting and commenting on the salient results obtained, let us note that preliminary calculations were carried out with different mesh sizes to ensure the independence of the solutions with respect to the mesh. It should be noted that all the results exhibited here correspond to the 100x100 mesh, the maximum difference between this and the other finer meshes(not shown here) being 0.3%.

4.1. *Re* effect on the *U*-velocity and fluid and porous medium temperatures

The U-contours (see Figure 2) are depicted for $Pr = 50, Re = 200$, $Ec = 0$ and $\varepsilon = 0.9$. At high porosity (= 0.9). It can be seen that the shape of the U -shaped contours is modified depending on A and St, thereby indicating the effect of the porosity. It should be specified that there is no viscous dissipation, Ec being zero.

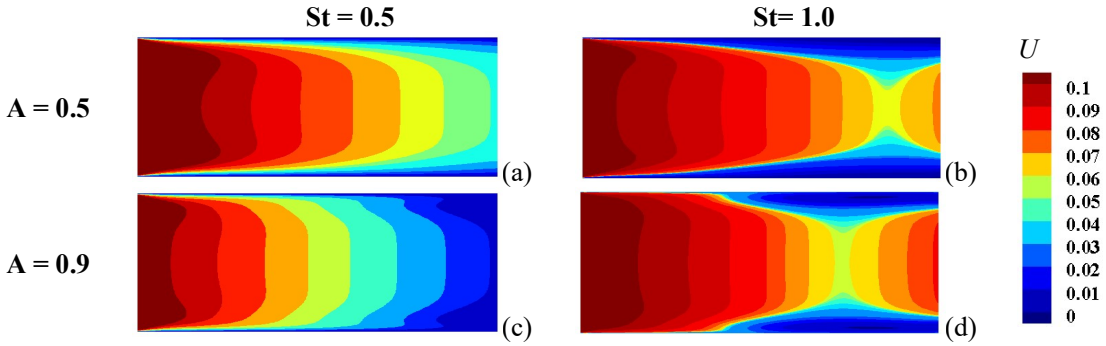

Figure 2: *Strouhal number and amplitude, A effects on U -contours during charging*

4.2. *St* and pulsating amplitude effects on solid-fluid differencetemperature

Figure 3 shows the temperature difference $(\Theta_f - \Theta_s)$ evolvement vs. the streamwise coordinate during the charging process parameterized by the porosity, pulse amplitude and St.

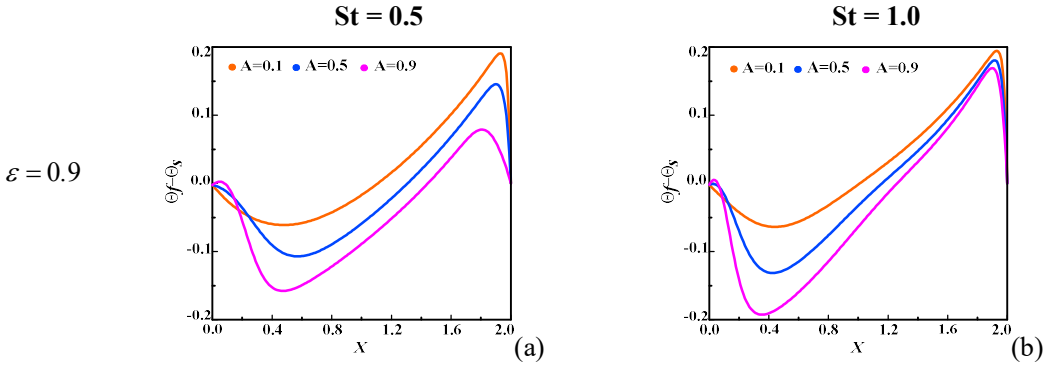

Figure3: *Strouhal,St, number and amplitude, A, effects on $\Theta_f - \Theta_s$ vs. X at Y = 0*

The profiles initially drop independently of A then rise inversely proportional from a critical value Xc close to the channel inlet to exhibit a maximum towards the outlet regardless of the

porosity. Besides, it appears from this figure that the LTNE condition is regarded as met throughout the channel whatever pulse amplitude and Strouhal number.

4.3. *St* and pulsating amplitude effects on liquid fraction and melt front

Figure 4 shows the liquid fraction evolution vs. the pulsation prametrized by St number and pulsating amplitude A.

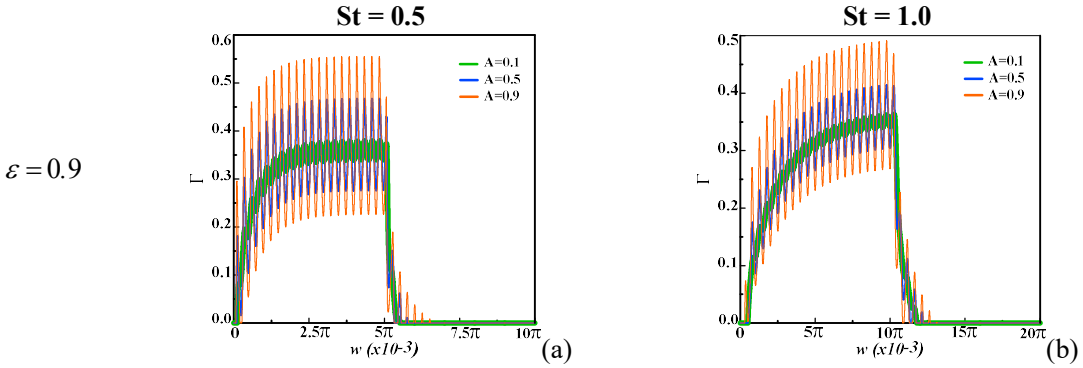

Figure 4: *Strouhal, St, number and amplitude, A, effects on the local* Γ *vs. the pulsation*

4.4. Melting frontevolvement

To inspect the effect of the parameters A and St, the melting front (phase field) evolvement is plotted in Figure 5 at $\varepsilon = 0.9$.

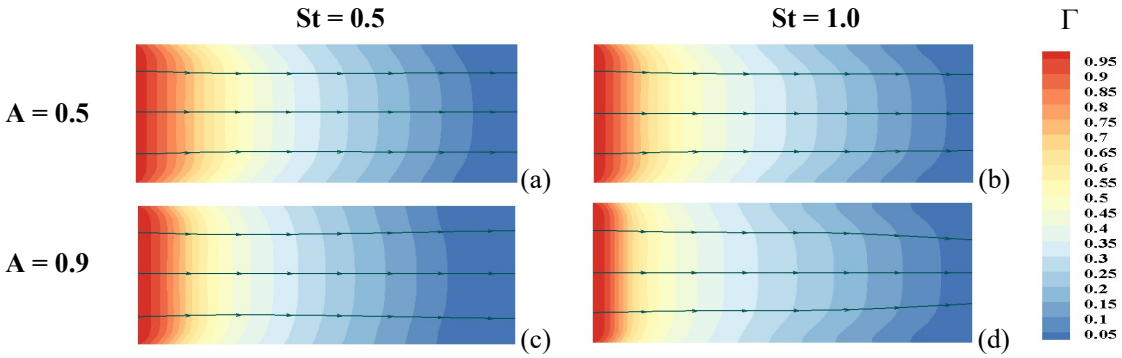

Figure 5: *Strouhal, St, number and pulsating amplitude, A, effects on the phase field and streamlines*

5. Conclusion

This paper deals with the simulation of an unsteady forced convection in a porous LHTES depicted by a straight channel, and subjected to an inlet flow modulation in the BGK-TLBM framework under the LTNE condition and without viscous dissipation.The flow and thermal fields inside the system were simulated using the Brinkman Forchmeyer's extended Darcy model and two-energy model.

The main results are exhibited in terms of velocity-contours, solid-fluid difference temperature, streamlines, and melt front progress during the charging (melting) process. Based on our findings, the main conclusions are as follows:

- A high porosity value (= 0.9) slows down the pulsating amplitude effect due to the medium's permeability.
- The temperature difference increases inversely with A whatever the St number.
- The St increase involves variations of velocity, temperature difference and phase field.

Next, we plan to focus on a wide range of porosities, pulse amplitudes, Reynolds numbers, and other relevant parameters. To sum up, an LBM simulation framework is an outstanding starting point for direct numerical simulations of porous LHTESs where both convective fluid flow and heat can be paramount.

References

[1] S. Marelli, M. Capobianco, Steady and pulsating flow efficiency of a waste-gatedturbocharger radial flow turbine for automotive application, *Energy*, 36 (2011) 459-465.

[2] Chang, S. W., Cheng, T. H, Thermal performance of channel flow with detached and attached pin-fins of hybrid shapes under inlet flow pulsation, *Int. J. Heat Mass Transf.*, 164, 120554.

[3] C.Y. Zhao, W. Lu, Y. Tian, Heat transfer enhancement for thermal energy storage using metal foams embedded within phase change materials (PCMs), *Solar Energy*, 84 (2010), 1402-1412.

[4] Y. Tian, C.Y. Zhao, A numerical investigation of heat transfer in phase change materials (PCMs) embedded in porous metals*, Energy*, 36 (2011), 5539-5546.

[5] Z. Deng, X. Liu, C. Zhang, Y. Huang, Y. Chen, Melting behaviours of PCM in porous metal foam characterized by fractal geometry. *Int. J. Heat Mass Transf.*, *113* (2017), 1031-1042.

[6] M.Ghalambaz, J. Zhang, Conjugate solid-liquid phase change heat transfer in heatsink filled with phase change material-metal foam *Int. J. Heat Mass Transf.*, 146(2020), 118832.

[7] M.Jafari, M.Farhadi, K.Sedighi, Convection heattransfer of SWCNT-nanofluid in a corrugatedchannelunderpulsatingvelocity profile. *Int. Commun. Heat Mass Transf.*, 67 (2015) 137-146

[8] G.F. Al-Sumaily, M.C. Thompson, Forced convection from a circular cylinder in pulsating flow with and without the presence of porous media, *Int. J. Heat Mass Transf.*, 61 (2013), 226-244.

[9] D.A. Nield, A. Bejan, Convection in Porous Media, 4th ed., Springer-Verlag, New York, 2013.

[10] R. Mabrouk, H. Dhahri, H. Naji, S. Hammouda, Z. Younsi, Lattice Boltzmann simulation of forced convection melting of a composite phase change material with heat dissipation through an open-ended channel. *Int. J. Heat Mass Transf.*, 2020, 153, 119606.

[11] V. Joshi,M K.Rathod, Constructal enhancement of thermal transport in metal foam-PCM composite-assisted latent heat thermal energy storage system*. Numer. Heat Tr A-Appl.*, 75(2019), 413-433.

[12] W. Zhao, D. France, W. Yu, T. Kim, D. Singh, Phase change material with graphite foam for applications in high-temperature latent heat storage systems of concentrated solar power plants, *Renewable Energy* , 69 (2014), 134-146.

[13] Y. S.Ranjbaran,S. J. Haghparast, M. H. Shojaeefard, G. R. Molaeimanesh, Numerical evaluation of a thermal management system consisting PCM and porous metal foam for Li-ion batteries. *J. Therm. Anal. Calorim.*, 2019, 1-23.

[14] X. Shan, X.-F. Yuan, H. Chen, Kinetictheoryrepresentation of hydrodynamics: a way beyond the Navier-Stokes equation, *J. Fluid Mech.*, 550(1) (2006), 413-441.

[15] Y. Gao, Y. Yu, L. Yang, Sh. Qin, G. Hou, Development of a coupledsimplifiedlattice Boltzmann method for thermal flows, *Comput. Fluids*, 229 (2021), 105042.

[16] R. Du, Z. Liu, A lattice Boltzmann model for the fractional advection-diffusion equation coupledwith incompressible Navier-Stokes equation, *Appl. Math. Lett.*, 101 (2020) 106074.

[17] Z Guo, T.S. Zhao, A lattice Boltzmann model for convection heat transfer in porous media, *Numer. Heat Transf. Part B*, 47(2) (2005), 157-177.

[18] Y.B. Tao, Y. You, Y.L. He, Lattice Boltzmann simulation on change heat transfer in metal foams/paraffin composite phase change material, *Appl. Therm. Eng.*, 93 (2016), 476-485.

Acknowledgements

The authors would like to thank the Artois University for its excellent initiatives helping the second author to complete scientific stays as part of his work on her PhD under the supervision of Prof. H. NAJI.